



Influence of the Crystallinity of Silver Nanoparticles on Their Magnetic Properties

Long Lin, Xiaogang Peng, Emilie Voirin, Bertrand Donnio, Mircea Rastei, Bertrand Vilenno, Jean-louis Gallani

► To cite this version:

Long Lin, Xiaogang Peng, Emilie Voirin, Bertrand Donnio, Mircea Rastei, et al.. Influence of the Crystallinity of Silver Nanoparticles on Their Magnetic Properties. *Helvetica Chimica Acta*, 2023, 106 (3), <10.1002/hlca.202200165>. <hal-04253834>

HAL Id: hal-04253834

<https://hal.science/hal-04253834v1>

Submitted on 23 Oct 2023

HAL is a multi-disciplinary open access archive for the deposit and dissemination of scientific research documents, whether they are published or not. The documents may come from teaching and research institutions in France or abroad, or from public or private research centers.

L'archive ouverte pluridisciplinaire **HAL**, est destinée au dépôt et à la diffusion de documents scientifiques de niveau recherche, publiés ou non, émanant des établissements d'enseignement et de recherche français ou étrangers, des laboratoires publics ou privés.



HAL Authorization

Influence of the Crystallinity of Silver Nanoparticles on their Magnetic Properties

Long LIN,^a Xiaogang PENG,^a Emilie Voirin,^b Bertrand DONNIO,^b Mircea V. RASTEI,^b Bertrand VILENO,^c Jean-Louis GALLANI ^{b*}

a. Center for Chemistry of Novel and High-Performance Materials, Department of Chemistry, Zhejiang University, Hangzhou 310027, People's Republic of China.

b. IPCMS, CNRS, Université de Strasbourg, 23 rue du Loess, BP43, 67034 Strasbourg cedex 2, France.

c. POMAM, Institut de Chimie de Strasbourg, UMR 7177. Université de Strasbourg, 1 rue Blaise Pascal, BP 296 R8, F-67008 Strasbourg Cedex

Dedication: To Professor Robert Deschenaux on the occasion of his retirement.

Abstract

The magnetic properties of noble-metal nanoparticles are a puzzling phenomenon, tentatively often explained as a size effect or a ligand effect. Many experimental studies performed to date have attempted to vary these readily available parameters without reaching a definitive conclusion. In an attempt at better understanding the role of core crystallinity on these magnetic properties we have compared the behaviour of silver nanoparticles, which were either single-crystalline or multi-twinned, of almost identical sizes and with the same ligand coating. Our results indicate that single-crystalline nanoparticles tend to behave as classical paramagnetic materials whereas multi-twinned ones exhibit a combination of para- and ferro-magnetic behaviours. Our hypothesis is that lattice defects within the core bear magnetic moments which couple via conduction electrons, with dipolar interactions also playing a local and macroscopic role.

Keywords: Nanoparticles, Magnetism, Crystallinity, Lattice defects

Introduction

There is a great body of research on the magnetic properties of silver and gold nanoparticles, both experimental and theoretical.^[1,2,3] Indeed, while up to the turn of the century these metals had been considered plain materials, they suddenly offered a surprisingly great amount of new properties when prepared in the form of nanocrystals. Research is now very active in fields as various as diagnosis,^[4,5] therapy,^[6,7] drug or gene delivery,^[8,9] catalysis,^[10,11] optics,^[12,13] sensing^[14,15] and imaging.^[16,17] Regarding the magnetic properties of these nanoparticles, the situation unfortunately bears similarities to the question of semiconductors in the 30's : are silver (or gold) nanoparticles indeed "magnetic".¹⁸ Experimental results are scattered, controversial, and so far no theory has been put forth which could explain all observations. Still, one has to remark that nanoparticles are not as simple as they seem. Most samples have been synthesized using processes far less precise than traditional organic/inorganic chemistry, leaving experimenters to investigate and try to understand batches of

$\sim 10^{16}$ nanoparticles, all differing in shape, faceting, crystallinity, number of atoms and/or ligands. The physical behaviours that are displayed by such variegated individuals necessarily cannot be homogeneous, efficiently preventing the observation of the usual structure/properties correlations that could help clarify the picture. This is even more true in the field of magnetism since not only do the characteristics of each NP differ from those of its neighbors but the inter-nanoparticle couplings also greatly vary, resulting in a wealth of macroscopic behaviours such as super-diamagnetism,^[19,20] ferromagnetism,^[3] spin glasses^[21] and –almost classically– paramagnetism. Even putting aside collective behaviors, theoretical studies that go beyond the over-simplistic model of a monodisperse batch of perfectly spherical NPs^[22] predict that the magnetic behaviour is indeed highly dependent on the diameter, and on the size dispersion.^[23]

The most common nanoparticles comprise a nanometric metal core stabilized by molecular ligands, covalently bond to the metallic surface or not, and it is today beyond experimental reach to accurately control the structure of the metal nanoclusters. The question of the crystallinity has therefore barely been addressed so far since it was also thought impossible to control.^[24] True, a handful of molecular clusters which have atomically precise composition and structure^[25] have been synthesized but most are barely nanoparticles in the true sense, lacking for example the hallmark plasmon resonance of *bona fide* silver or gold nanoparticles.^[26] Magnetometry and DFT studies have been performed on one such atomically precise cluster, $\text{Au}_{25}(\text{SCH}_2\text{CH}_2\text{Ph})_{18}$, and a variety of magnetic behaviours has been observed, the outcome of the measurements depending on "*a very delicate balance of factors*" : atomic control of composition, charge state, crystallinity, experimental conditions.^[27] We shall not further consider these materials here. Going back to regular nanoparticles, a synthetic procedure has recently been published which enables the synthesis of silver NPs that are single-crystalline (SC) or multi-twinned (MTW) and almost mono-disperse.^[28] We have therefore endeavored to compare the magnetic properties of these two sorts of nanoparticles, in view of better understanding the influence of crystalline quality on the magnetic properties. Our initial work hypothesis was that the single-crystalline particles would be the perfect candidates for sustaining the electronic persistent currents that some of us had suggested as being at the origin of Au magnetic properties.^[29] To our surprise, as will be seen hereafter, we observed the opposite.

Results and Discussion

Let us start with the comparison of SC vs. MTW nanoparticles. Figure 1 compares the isothermal magnetization curves of all samples at 300K and 4K. The behaviours of both types of NPs is obviously not the same. At the first order, just from the shape of the magnetization curves, single-crystalline NPs display a globally diamagnetic response whereas multi-twinned NPs exhibit either a ferro- or paramagnetic one.

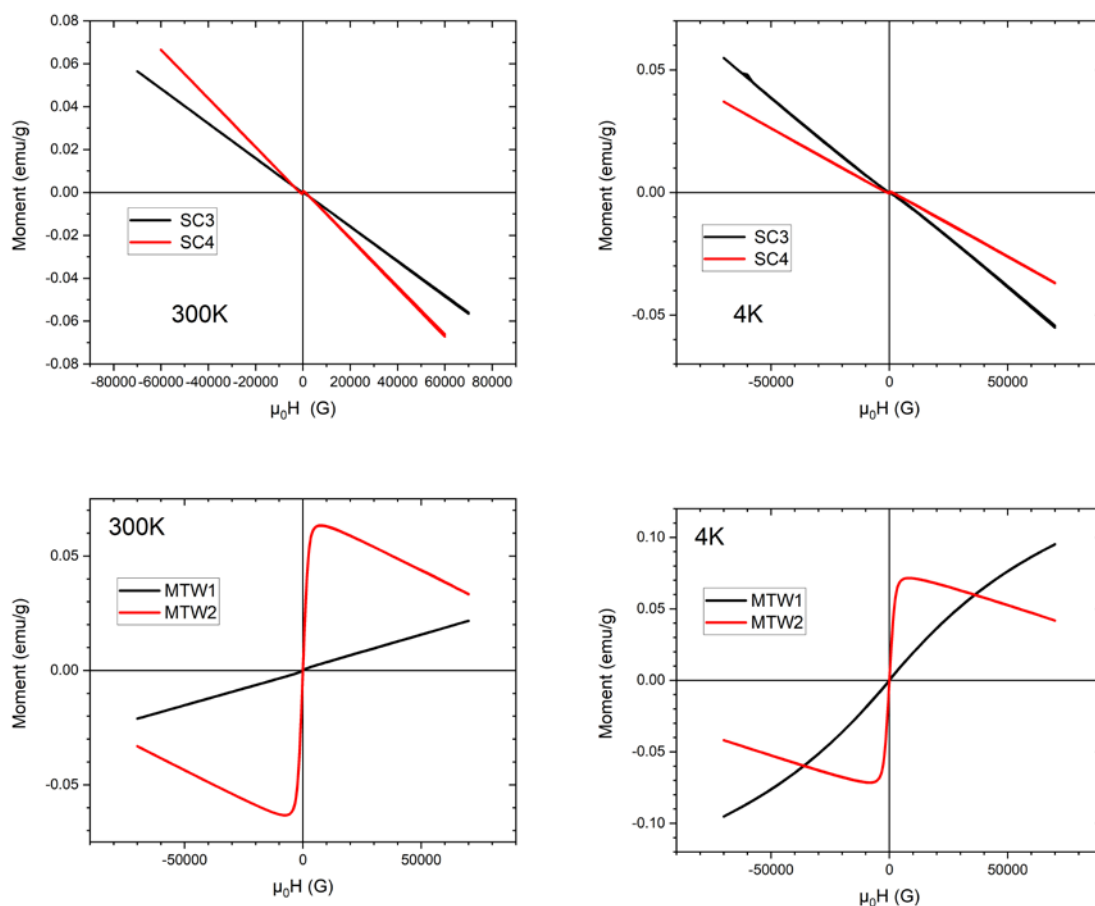


Figure 1. Top: Magnetization vs. applied field of single-crystalline samples (SC3 and SC4) at room temperature (left) and 4K (right). Bottom: Magnetization vs. applied field of multi-twinned samples (MTW1 and MTW2) at room temperature (left) and 4K (right). See also Supplementary Information for details at low fields.

Within each class though, samples do not behave exactly in the same way. SC3 and SC4 both display hysteretic behaviours but in low fields, the magnetization curve of SC4 has a sigmoidal form, which is not seen in the curve of SC3. MTW1 and MTW2 also display hysteretic behaviours but whereas the magnetization of MTW1 increases smoothly up to the maximum applied field (7T), the magnetization of MTW2 has a sigmoidal form, with a sharp increase up to a field of *ca.* 0.65T before decreasing almost linearly. The most obvious reason we see for explaining these minor differences is that the synthetic procedure produces batches that are dominantly either mono-crystalline or multi-twinned but certainly not 100% perfect, macroscopic chemistry has its limits. Hence, the features of each type of clusters, SC or MTW, are blurred by the unavoidable presence of clusters of the opposite type as “impurities” and, in the case of MTW clusters, the nature and number of defects are obviously totally beyond our control. If we posit that SC clusters are diamagnetic, the small sigmoidal shape of SC4 magnetization curve can be ascribed to the presence of a few MTW clusters, which we tend to consider as being para- or ferro-magnetic. Similarly, the two batches of MTW clusters cannot be strictly identical, and they obviously will differ in the nature and number of defects that they contain on average.

As is usual for nanoparticles, the thermal behaviour of the samples has also been probed by recording FC/ZFC curves (Figure 2). Here again each one of the four samples displays a singular behavior: low temperature divergence (MTW1), smooth decrease with temperature (MTW2), smooth increase (SC3),

and broad maximum (SC4). For all samples, FC and ZFC curves look identical, differing mostly by a small vertical shift. The mere aspect of these FC/ZFC curves implies that these silver clusters are not “magnetic nanoparticles” in the traditional sense like *e.g.*, ferrite nanoparticles.

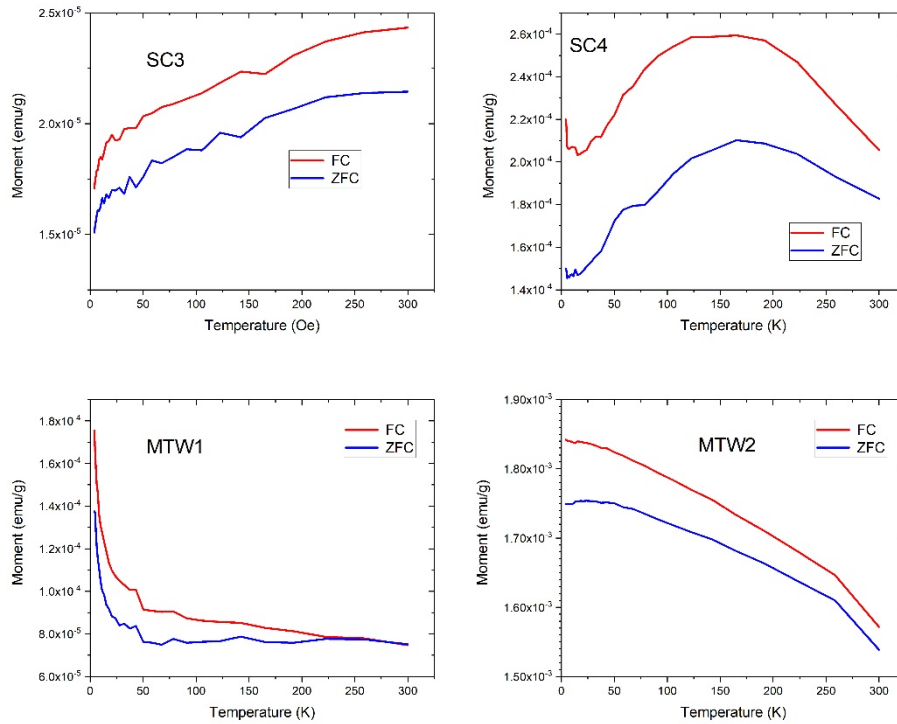


Figure 2. FC/ZFC curves for the monocrystalline samples (Top) and-for the multi-twinned samples (Bottom).

Similarly, the shape of the χ plots, *i.e.* inverse of the magnetic susceptibility χ plotted versus temperature (Curie plots, Figure 3) also reveal a non-traditional behaviour. For traditional magnetic materials a more or less linear behaviour is observed for the Curie plots, which is clearly not the case here. Departure from a linear temperature dependence of $1/\chi$ can be observed for reasons such as superparamagnetism, Van Vleck effect, non-localized moments or low dimensionality. In the case of intrinsically magnetic nanoparticles (*e.g.* Fe or ferrites) a common reason is when there is a distribution of relaxation times.³⁰ On the one hand these observations imply that we are not dealing with traditional materials, and on the other hand this singular behaviour excludes the presence of any paramagnetic impurities (*e.g.* Fe). Electron spin resonance experiments (ESR) have also been performed and all samples were ESR-silent. On the basis of the experimental data, we offer the following as our work hypothesis: single-crystalline silver nanoparticles are diamagnetic, multi-twinned nanoparticles are para- or ferro-magnetic, with any eventual hypothetical blocking temperature being higher than 300K. The fact that the shape of the Curie plot differs from sample to sample, beyond what could be reasonably ascribed to statistical fluctuations, is indicative of some more intrinsic reason. We believe that this supports our suggestion that the magnetic behaviour of the silver nanoparticles stems from the lattice defects in their cores, which is inherently uncontrollable and very variable from particle to particle and henceforth from batch to batch. Attempts at fitting these curves have failed or returned totally unrealistic values for the parameters. Beyond the fact that the shape of the curves is singular, the range of values for $1/\chi$ is rather small (factor of 2 at most), preventing the adjustment to a regular Curie-Weiss law, even if a constant χ_0 is added.^[31]

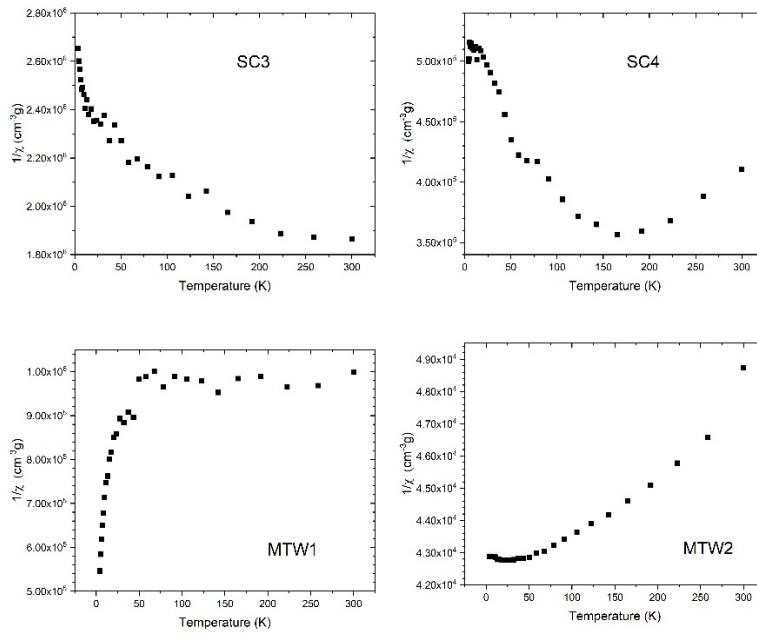


Figure 3 Inverse of the magnetic susceptibility vs. temperature (Curie plot) for all samples, as labelled. A straight line is expected for magnetic samples obeying Curie's law, $\chi=C/T$ or Curie-Weiss law, $\chi=C/(T-T_c)$. Samples discussed here do not display such typical behaviours.

Last, all this is further confirmed by the χT plots, given in Figure 4. These plots greatly differ from traditional ones, precluding the unambiguous attribution of these thermal behaviours to any class of magnetism.

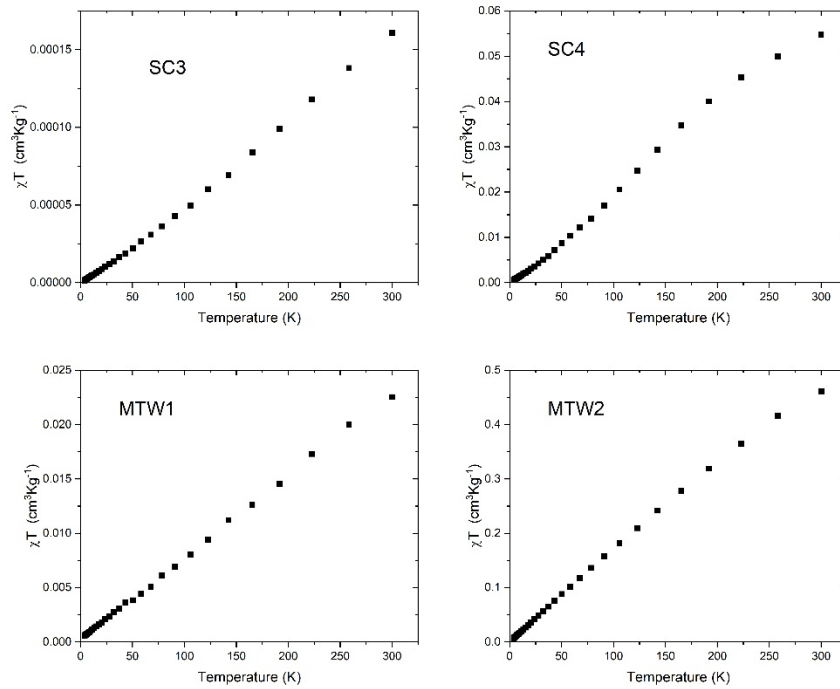


Figure 4. χT plots of all samples, as labelled. Top: monocrystalline samples. Bottom: multi-twinned samples. None of the curves can be related to the behaviour of traditional magnetic materials (e.g. ferro-, para- or diamagnetic)

Discussion

There are examples of materials becoming magnetic upon presence of extrinsic (e.g. Fe atoms in Pt) or intrinsic defects. The subject is heavily documented in the case of oxides, nitrides and semiconductors, for thin films or nano-objects (e.g. nanoparticles, tubes, ribbons, ...).^[32,33,34] The most common cases are oxygen or nitrogen vacancies. Carbon vacancies or “dangling bonds” in materials such as graphene are also known to induce magnetism.^[35] A very relevant study has reported the appearance of magnetism in plutonium due to radiation self-damage.^[36] ^{239}Pu decays into ^{235}U by emission of an α -particle. The ^{235}U atom recoils energetically and doing so creates defects (vacancies, interstitial atoms,...) in the plutonium lattice. Bulk plutonium is not magnetic but becomes much more so with time, as the number moment-bearing lattice defects increases.^[37] We reckon that the situation is similar with our silver nanocrystals.

Let us start the discussion with the FC/ZFC curves since these are traditionally recorded when dealing with magnetic nanoparticles. The ZFC magnetization curve is recorded by measuring the magnetization at stepwise increasing temperatures in a small applied field ($\mu_0 H = 75$ G in the present case) after cooling the sample in zero field from high temperature. The FC magnetization curve is recorded by measuring magnetic moment during the cooling process while the same small field is applied. In the case of regular homogeneous nanoparticles, the FC/ZFC curves have typical shapes^[38] and in particular the ZFC curve usually displays a clear maximum at the so-called blocking temperature. Still, when the blocking temperature is above the explored range, or in the case of inhomogeneous samples having a large dispersion of the size or properties of the nanoparticles, the FC/ZFC curves may display atypical shapes. If for example there is a large distribution of blocking temperatures with none dominating, no clear maximum can be seen in the ZFC curve.^[20] In the case of interacting lower dimensionality structures, e.g. chains of nanoparticles with dipolar interactions, atypical FC/ZFC curves are also observed and the two curves become indistinguishable.^[39] Last, FC/ZFC curves having some resemblance with ours have also been reported for ferrite nanoparticles where two magnetic sublattices interact and compete^[40] but this explanation can most certainly be ruled out here as all Ag atoms have a similar coordination. In our case on the contrary, what may worsen the situation is that the exact magnetic nature of each particle differs from that of the others and probably differs from the usually observed paramagnetism. The minimum information we can extract from our data is that the systems have a ferromagnetic ground state since the ZFC curves do not drop to zero at low temperatures.^[41]

We posit that perfect Ag nanoparticles would be diamagnetic. We also hypothesize that the atoms around a vacancy acquire a magnetic moment through an increased localization of their $4d$ or $5d$ electrons. The asymmetric local environment at a defect can induce some imbalance in the s -band which favors emergence of a spin, as put forth by the authors of reference 36 discussing “how a spinless vacancy can induce magnetic moments on the surrounding lattice” in pure plutonium. Single-crystalline nanoparticles magnetization curves are indeed almost purely diamagnetic ones,^[42] the hysteresis that is observed being very weak. On the contrary, multi-twinned nanoparticles clearly display soft ferromagnetism, the magnetic moment always has the same sign as the applied magnetic field. Coercive fields remain small, comparable in fact to the one of defectless nanoparticles, which we believe indicates that some defect-bearing nanoparticles are present in the SC samples.

Considering sample MTW2, its magnetic moment at 300K reaches a maximum of $0.06 \text{ emu} \cdot \text{g}^{-1}$ (Figure 2), which is roughly $40 \mu_B$ per particle.^[43] For the sake of discussion, let us assume that one lattice defect generates $1 \mu_B$. This implies that there are on average 40 such defects per particle, each one within a

volume of $\sim 15\text{nm}^3$ (880 atoms). Two defects therefore sit on average 3nm apart, meaning there are *ca.* 20 Silver atoms in between. Given these numbers, one may consider that some exchange coupling via conduction electrons could easily occur within a single particle since RKKY (Ruderman–Kittel–Kasuya–Yosida interaction) exchange typically occurs at distances of a few nanometers. These figures are just average values, some nanoparticles bear a much larger moment whereas others may have none. A very broad distribution of the magnetic properties is expected. Should for example the nanoparticles be superparamagnetic, this distribution would lead to atypical FC-ZFC curves. In any case, the weak ferromagnetism that is observed at room temperature requires exchange coupling or anisotropy. Even though defects and magnetic centers can exhibit anisotropy, crystalline anisotropy can easily be ruled out since there is no easy axis and coercive fields are very weak. We mean here that the nanoparticle as a whole cannot be magnetically anisotropic, neither are there Weiss domains or Bloch walls. This said, it has been suggested that a large (*giant*, in the original paper) anisotropy may arise when localized charges or spins trap conduction electrons in surface orbits with a large angular momentum.⁴⁴ It nevertheless seems that there are localized moments, which are coupled while others are not and it is therefore difficult to understand which parameter could influence this elusive coupling. Other types of ferromagnetic coupling resulting from magnetic centers being indirectly coupled, such as Griffiths phase or Kondo systems, can *a priori* be excluded since they would display signature of the thermal behaviors of their magnetization, not observed here.

It may seem pertinent to try annealing the nanoparticles and check whether the MTW ones lose their magnetic properties and the SC ones become purely diamagnetic. This has not been attempted. We know that heating the nanoparticles up to 110°C has no effect on their magnetic properties at room temperature which remain unchanged. Heating the samples at higher temperatures within our SQUID is not possible, and heating a sample ex-situ would imply removing it from its gelatin holder before putting back into the SQUID which is a lot of manipulation and could bring spurious effects. In any case the organic coating of the nanoparticles starts decomposing irreversibly at *ca.* 200°C.

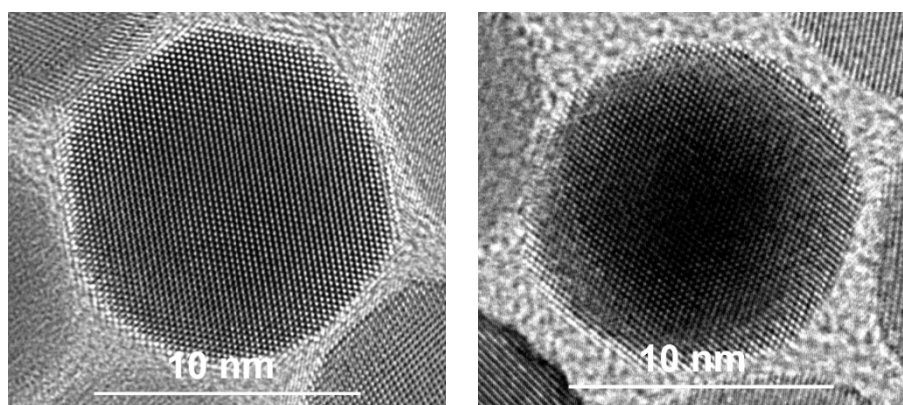
Considering now the macroscopic behavior, there is a need to understand how the nanoparticles interact. Each particle is coated with organic ligands *ca.* 20Å thick, mostly made of alkyl chains. They are therefore electrically insulated from each other. Tunneling processes through 40Å of non-conductive molecules can reasonably be excluded.^[45] A large Kondo effect has been observed in assemblies of gold nanoparticles but the nanoparticles were linked by single 1,4-butanedithiol molecules.^[46] Any collective (macroscopic) magnetic behavior can consequently only occur via dipolar interactions. Such dipolar interactions have been shown to be effective, even for nanoparticles in solution, that is at large distances.^[47] A collective behavior termed super-ferromagnetism has been suggested to take place in systems where small clusters or islands bearing macro-moments would be coupled *via* dipolar interactions.^[48,49] Moments around $100\mu_B$ and distances of a few nanometers are indeed enough for super-ferromagnetism to persist at room temperature. Anyway, for dipolar couplings at room temperature, it is essential that clusters of nanoparticles with coupled moments exist.^[50] The value of $40\mu_B$ for the moment of MTW2 is an average over the whole sample. It is therefore expected that some nanoparticles will bear a larger moment whereas others may bear none. The possible role played by such “non-magnetic” nanoparticles also remains unknown. In the case of MTW2 this is, in fact, the only possibility for ferromagnetism at room temperature. This is because magnetic moments of $40\mu_B$ per nanoparticle in a system where they are separated by *ca.* 11nm would yield an ordering temperature in the milli-kelvin range.⁵¹

Conclusions

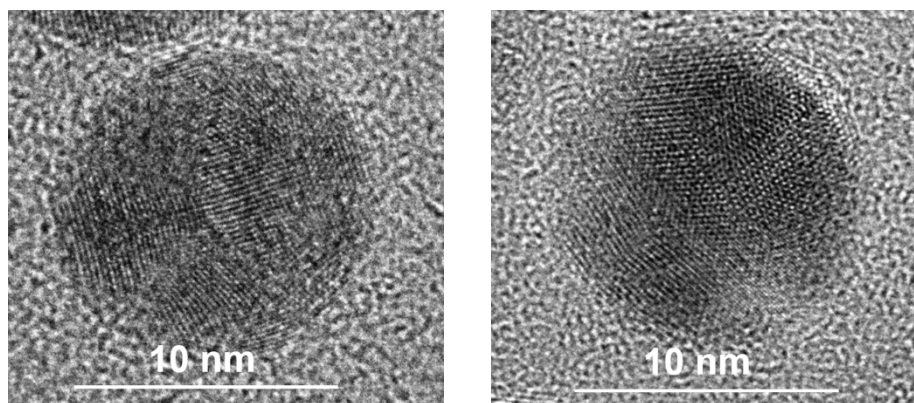
The problem with nanoparticles magnetism is two-pronged: why should noble metal cluster become magnetic and why are the observations so scattered? Magnetometry measurements presented here show that multitwinned Ag nanoparticles display magnetic behaviours strongly deviating from those of monocrystalline ones. These data at least indicate a relationship between crystalline quality and magnetic properties. Defects appear in an uncontrolled way and this constitutes a good explanation for the variability of experimental results. Regarding the localization of magnetic moments on defects, more evidences could maybe be brought by Lorentz electron microscopy on isolated nanoparticles, eventually with lattice defects being created in situ by the electron flux. Defect-induced magnetism is certainly not limited to Ag nanoparticles and could most probably also explain the poorly understood magnetic properties of nanoparticles made of other metals such as Cu, Au, Pt or Pd. Magnetism could of course also have other origins, such as those already reported in the literature. An interplay between defect-induced magnetism and, *e.g.* surface- or ligand-induced magnetism is certainly possible and this could explain some unusual observations. The hypothesis that we present here would nevertheless explain the large variety of experimental observations reported by the various experimenters and as such, deserves attention.

Experimental section

Silver nanoparticles have been synthesized following the procedure already published.²⁷ Nanoparticle synthesis is known for being poorly reproducible, different batches displaying similar but never quite identical properties. Four synthetic batches have been prepared, at the same time, in the same laboratory, by the same person, using reactants from the same pots. Two samples of multi-twinned NPs, MTW1 and MTW2, with a mean diameter of 11.4nm and 10.9nm, respectively, and two samples of single-crystalline NPs, SC3 and SC4, also with mean diameters of 11.4nm and 10.9nm, respectively. Representative images are given in figure 6. Dispersion on the diameters was $\pm 0.5\text{nm}$ for each batch, determined by computerized statistical analysis on *ca.* 1000 nanoparticles, from several TEM pictures. A 10.5nm diameter silver nanoparticle comprises *ca.* 35500 atoms. The notion of molecular weight is ill-suited for such objects but an estimate would be *ca.* $4.2 \times 10^6 \text{g/Mol}$ for ligand-coated nanoparticles, just to set the order of magnitude. Electronic configuration of Silver is [Kr] $4d^{10} 5s^1$.



(a) Single crystalline Ag nanoparticles



(b) Multitwinned Ag nanoparticles

Figure 6. HR TEM images of (a) single-crystalline and (b) multitwinned Ag nanoparticles

Magnetometry has been performed with a Quantum Design MPMS SQUID magnetometer. A small amount of each sample (*ca.* 20mg) was set and sealed into a gelatin holder, placed inside a plastic straw. Measurements were taken in the "comfort zone" of the SQUID (*i.e.* enough signal) and adjustments proceeded without problems. Each point was measured three times and the values averaged. The presented curves display all data points recorded, none was removed. Magnetic response of an empty gelatin holder placed inside an identical straw has been measured as purely diamagnetic and the resulting small magnetic moment has been considered when analyzing the behaviour of the various NPs. No correction for the diamagnetism of the ligand shell of the NPs was applied. Magnetization curves have been recorded at room temperature and at 4K. Thermal behaviour of some samples has also been probed by recording FC/ZFC magnetization curves (see ESI). Depending on each sample and its magnetic history, the first magnetization branch of the magnetization curves is not always seen or, when seen, does not always starts at the origin. Given the amorphous nature of the samples this bears no significance.

Transmission Electron microscopy (TEM) was performed on a TOPCON LaB₆ microscope from JEOL.

Supplementary Material Description

Additional figures can be found in the supplementary materials. Comparison of M(H) for SC3 and bulk silver, M(H) curves for all samples at low fields, tentative fit of M(H) for sample MTW2 with a Brillouin curve.

Authors contribution

LL synthesized the nanoparticles (SC and MTW) and performed the electronic microscopy characterization, under the supervision of XP. EV performed some complementary syntheses and analyses. BV was in charge of the ESR experiments. JLG performed the magnetometry and analysis of the data. BD, MVR and JLG conceived the experiment and wrote the manuscript.

Acknowledgments

MVR, BD and JLG acknowledge funding received from EOARD (FA8655-13-1-3001) and ANR (ANR-14-OHRI-008; ANR-12-BS10-00301). The TEM platform of IPCMS is gratefully acknowledged for providing access to the JEOL LaB6 microscope. The magnetometry platform is acknowledged for access to the SQUID magnetometer.

References

- ¹ S. Trudel, Unexpected magnetism in gold nanostructures: making gold even more attractive, *Gold Bull.* **2011**, *44*, 3-13.
- ² G.L. Nealon, B. Donnio, R. Greget, J.-P. Kappler, E. Terazzi, J.-L. Gallani, Magnetism in gold nanoparticles, *Nanoscale* **2012**, *4*, 5244-5258.
- ³ J.S. Garitaonandia, M. Insausti, E. Goikolea, M. Suzuki, J.D. Cashion, N. Kawamura, H. Ohsawa, I.G. de Muro, K. Suzuki, F. Plazaola, T. Rojo, Chemically induced permanent magnetism in Au, Ag, and Cu nanoparticles: localization of the magnetism by element selective techniques, *Nano Lett.* **2008**, *8*, 661-667.
- ⁴ T.S. Siddiqui, A. Jani, F. Williams, R.N. Muller, L. van der Elst, S. Laurent, F. Yao, Y.Z. Wadghiri, M.A. Walters, Lanthanide complexes on Ag nanoparticles: Designing contrast agents for magnetic resonance imaging, *J. Coll. Interf. Sci.* **2009**, *337*, 88-96.
- ⁵ W. Zhou, X. Gao, D. Liu, X. Chen, Gold nanoparticles for in vitro diagnostics, *Chem. Rev.* **2015**, *115*, 10575-10636.
- ⁶ B.H. Jun, M.S. Noh, J. Kim, G. Kim, H. Kang, M.S. Kim, Y.T. Seo, J. Baek, J.H. Kim, J. Park, S. Kim, Y.K. Kim, T. Hyeon, M.H. Cho, D.H. Jeong, Y.S. Lee, Multifunctional silver-embedded magnetic nanoparticles as SERS nanoprobes and their applications, *Small* **2010**, *6*, 119-125.
- ⁷ M.F. Hornos Carneiro, F. Barbosa Jr, Gold nanoparticles: A critical review of therapeutic applications and toxicological aspects, *J. Toxicol Environ Health B Crit. Rev.* **2016**, *19*, 129-148.
- ⁸ D. Dutta, A. Chattopadhyay, S.S. Ghosh, Cationic BSA templated Au-Ag bimetallic nanoclusters as a theranostic gene delivery vector for hela cancer cells, *ACS Biomater. Sci. Eng.* **2016**, *2*, 11.
- ⁹ P. Ghosh, G. Han, M. De, C. K. Kim, V. M. Rotello, Gold nanoparticles in delivery applications, *Advanced Drug Delivery Reviews* **2008**, *60*, 11, 1307-1315
- ¹⁰ H. Veisi, S.B. Moradi, A. Saljooqi, P. Safarimehr, Silver nanoparticle-decorated on tannic acid-modified magnetite nanoparticles (Fe₃O₄@TA/Ag) for highly active catalytic reduction of 4-nitrophenol, rhodamine B and methylene blue, *Mat. Sci. Eng. C* **2019**, *100*, 445-452.
- ¹¹ A. Corma, H. Garcia, Supported gold nanoparticles as catalysts for organic reactions, *Chem. Soc. Rev.* **2008**, *37*, 2096-2126.
- ¹² L. Wang, C. Clavero, Z. Huba, K.J. Carroll, E.E. Carpenter, D.F. Gu, R.A. Lukaszew, Plasmonics and enhanced magneto-optics in core-shell Co-Ag nanoparticles, *Nano Lett.* **2011**, *11*, 1237-1240.
- ¹³ V.A. Ogarev, V.M. Rudoi, O.V. Dement'eva, Gold nanoparticles: synthesis, optical properties, and application, *Inorg. Mater. Appl. Res.* **2018**, *9*, 134-140.
- ¹⁴ H. Li, W.B. Qiang, C.Z. Wang, M. Vuki, D.K. Xu, Ultrasensitive and fast fluorescent bioassay based on fluorescence enhancement of silver nanoparticles, *Analyst* **2013**, *138*, 7376-7383.
- ¹⁵ G. Zhang, Functional gold nanoparticles for sensing applications, *Nanotechnol Rev.* **2013**, *2*, 269-288.
- ¹⁶ O.S. Wolfbeis, An overview of nanoparticles commonly used in fluorescent bioimaging, *Chem. Soc. Rev.* **2015**, *44*, 4743-4768.
- ¹⁷ M.M. Mahan, A.L. Doiron, Gold nanoparticles as X-ray, CT, and multimodal imaging contrast agents: formulation, targeting, and methodology, *Hindawi J. Nanomater.* **2018**, Article ID 5837276.
- ¹⁸ G. Busch, Early history of the physics and chemistry of semiconductors-from doubts to fact in a hundred years, *Eur. J. Phys.* **1989**, *10*, 254.
- ¹⁹ P.G. Van Rhee, P. Zijlstra, T.G.A. Verhagen, J. Aarts, M.I. Katsnelson, J.C. Maan, M. Orrit, P.C.M. Christianen, Giant magnetic susceptibility of gold nanorods detected by magnetic alignment, *Phys. Rev. Lett.* **2013**, *111*, 127202.
- ²⁰ Y. Raju, P. Krishnamurthi, P.L. Paulose, P.T. Manoharan, Substrate-free copper nanoclusters exhibit super diamagnetism and surface based soft ferromagnetism, *Nanoscale* **2017**, *9*, 17963-17974.
- ²¹ W.C. Huang, J.T. Lue, Spin-glass properties of metallic nanoparticles conducted by quantum size effects, *Phys. Rev. B* **1999**, *59*, 69-72.
- ²² The legendary « spherical cow in a vacuum » of theoreticians.
- ²³ M. Gómez Vilorio, G. Weick, D. Weinmann, R.A. Jalabert, Orbital magnetism in ensembles of gold nanoparticles, *Phys. Rev. B* **2018**, *98*, 195417. See for example Figure 2.
- ²⁴ Putting aside DFT calculations on few-atoms clusters which we do not consider here.
- ²⁵ I. Chakraborty, T. Pradeep, Atomically precise clusters of noble metals: emerging link between atoms and nanoparticles, *Chem. Rev.* **2017**, *117*, 8208-8271.
- ²⁶ N.A. Sakthivel, M. Stener, L. Sementa, A. Fortunelli, G. Ramakrishna, A. Dass, Au₂₇₉(SR)₈₄: The smallest gold thiolate nanocrystal that is metallic and the birth of plasmon, *J. Phys. Chem. Lett.* **2018**, *9*, 1295-1300.
- ²⁷ M. Agrachev, A. Antonello, T. Dainese, M. Ruzzi, A. Zoleo, A. Aprà, N. Govind, A. Fortunelli, L. Sementa, F. Maran, Magnetic ordering in gold nanoclusters, *ACS Omega* **2017**, *2*, 2607-2617.
- ²⁸ L. Lin, M. Chen, H. Qin, X. Peng, Ag nanocrystals with nearly ideal optical quality: synthesis, growth mechanism, and characterizations, *J. Am. Chem. Soc.* **2018**, *140*, 17734-17742.
- ²⁹ R. Gréget, G.L. Nealon, B. Vilen, P. Turek, C. Mény, F. Ott, A. Derory, E. Voirin, E. Rivière, A. Rogalev, F. Wilhelm, L. Joly, W. Knafo, G. Ballon, E. Terazzi, J.-P. Kappler, B. Donnio, J.-L. Gallani, Magnetic properties of gold nanoparticles: a room-temperature quantum effect, *ChemPhysChem* **2012**, *13*, 3092-3097.
- ³⁰ S.A. Majetich, M. Sachan, Magnetostatic interactions in magnetic nanoparticle assemblies: energy, time and length scales, *J. Phys. D: Appl. Phys.* **2006**, *39*, R407. See for example Figure 3.

- ³¹ S. Mugiraneza, A. M. Hallas, Tutorial: a beginner's guide to interpreting magnetic susceptibility data with the Curie-Weiss law, *Commun. Phys.* **2022**, *5*, 95.
- ³² A. Sundaresan, C.N.R. Rao, Ferromagnetism as a universal feature of inorganic nanoparticles, *Nano Today* **2009**, *4*, 96-106.
- ³³ S. Ning, P. Zhan, Q. Xie, W.P. Wang, Z.J. Zhang, Defects-driven ferromagnetism in undoped dilute magnetic oxides: a review, *J. Mater. Sci. Technol.* **2015**, *31*, 969-978.
- ³⁴ S. Zhou, X. Chen, Defect-induced magnetism in SiC, *J. Phys. D: Appl. Phys.* **2019**, *52*, 393001.
- ³⁵ N. Sethulakshmi, A. Mishra, P.M. Ajayan, Y. Kawazoe, A.K. Roy, A.K. Singh, C.S. Tiwary, Magnetism in two-dimensional materials beyond graphene, *Materials Today* **2019**, *27*, 107-122.
- ³⁶ S. K. McCall, M. J. Fluss, B. W. Chung, M. W. McElfresh, D. D. Jackson, G. F. Chapline, Emergent magnetic moments produced by self-damage in plutonium, *PNAS* **2006**, *103*, 17179-17183.
- ³⁷ Annealing the sample allows the lattice to recover its integrity, the magnetic susceptibility goes then back to its initial value, which proves that lattice defects are indeed at the origin of the magnetism.
- ³⁸ A. Demortière, P. Panissod, P. Pichon, G. Pourroy, D. Guillon, B. Donnio, S. Bégin-Colin, Size-dependent properties of magnetic iron oxide nanocrystals, *Nanoscale* **2011**, *3*, 225-232.
- ³⁹ D. Serantes, D. Baldomir, M. Pereiro, B. Hernando, V.M. Prida, J.L. Sánchez Llamazares, A. Zhukov, M. Ilyn, J. González, Magnetic ordering in arrays of one-dimensional nanoparticle chains, *J. Phys. D: Appl. Phys.* **2009**, *42*, 215003.
- ⁴⁰ I.S. Lyubutin, S.S. Starchikov, A.O. Baskakov, N.E. Gervits, C.-R. Lin, Y.-T. Tseng, W.-J. Lee, K.-Y. Shih, Exchange-coupling of hard and soft magnetic sublattices and magnetic anomalies in mixed spinel $\text{NiFe}_{0.75}\text{Cr}_{1.25}\text{O}_4$ nanoparticles, *J. Magnetism Magnetic Mater.* **2018**, *451*, 336-343.
- ⁴¹ Noble metals (Au, Ag, Pt, Cu...) weakly diluted with transition metal ions are the physical drosophile of studies on spin glasses. We could consider that our suggestion for the origin of magnetism in Au and Ag nanoparticles, namely magnetic centres RKKY-coupled, could indeed form a spin glass. We believe that this can be ruled out as the thermal variation of the susceptibility of spin glasses presents a typical cusp which is never seen here. See for example: K. Binder, A.P. Young, Spin glasses: Experimental facts, theoretical concepts, and open questions, *Rev. Mod. Phys.* **1986**, *58*, 801.
- ⁴² Even though the diamagnetic susceptibility of these particles is greater (in absolute value) than that of solid silver, which is another open question.
- ⁴³ To no avail, we tried adjusting the behaviour of the magnetization of MTW2 sample with theoretical laws (see electronic supplementary information).
- ⁴⁴ A. Hernando, P. Crespo, M.A. Garcia, E. Fernandez-Pinel, J. de la Venta, A. Fernandez, S. Penades, Giant magnetic anisotropy at the nanoscale: Overcoming the superparamagnetic limit, *Phys. Rev. B.* **2006**, *74*, 052403.
- ⁴⁵ K. Slowinski, R. V. Chamberlain, C. J. Miller, M. Majda, *J. Am. Chem. Soc.* **1997**, *119*, 11910-11919.
- ⁴⁶ M. Tie, S. Gravelins, M. Niewczas, A. Dhirani, Large Kondo effect in assemblies of Au nanoparticles linked with alkanedithiol electron bridges, *Nanoscale* **2019**, *11*, 5395-5401.
- ⁴⁷ O. Kovalenko, M. Vomir, B. Donnio, J. L. Gallani, and M. V. Rastei, Chiro-magnetoptics of Au and Ag Nanoparticulate Systems, *J. Phys. Chem. C* **2020**, *124*, 21722-21729.
- ⁴⁸ S. Mørup, M. Fougat Hansen, C. Frandsen, Magnetic interactions between nanoparticles, *Beilstein J. Nanotechnol.* **2010**, *1*, 182-190.
- ⁴⁹ S. Bedanta, T. Seki, H. Iwama, T. Shima, K. Takanashi, Superferromagnetism in dipolarly coupled $L1_0$ FePt nanodots with perpendicular magnetization, *Appl. Phys. Lett.* **2015**, *107*, 152410.
- ⁵⁰ P. Panissod, M. Drillon, Magnetic ordering due to dipolar interaction in low dimensional materials, in « Magnetism: molecules to materials IV », Eds. J.S. Miller and M. Drillon, Wiley-VCH, Weinheim, **2003**.
- ⁵¹ It has been suggested to us that diluting the sample in eicosane could provide some insight on the long-range interparticle interactions. We once did try dilution in eicosane with another sample (gold nanoparticles) and did not see any significant behaviour change, except for a weakening of the amplitude of the measured signal, the behaviour remaining ferromagnetic-like. We did not try eicosane dilution in the present study. Rather than magnetic nanoparticles interacting via dipolar interactions our view is more of intra-particular interaction. As said in the text, it would be possible that some particles (or small clusters) bear a large moment ($>100\mu\text{B}$) or that some clusters form. It is not obvious that upon dilution those clusters would break down.

1) Comparison of SC3 with bulk silver

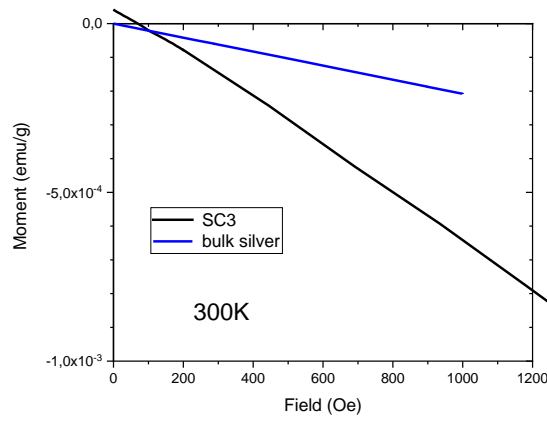


Figure S1. Measured susceptibility of a small silver cylinder (3mm diameter, length 3.3mm): $\chi = -2.08 \times 10^{-7}$ emu/g (or $\chi = -2.61 \times 10^{-9}$ m³kg⁻¹). The value compares reasonably with the literature values: $\chi = -1.89 \times 10^{-7}$ emu/g or $\chi = -2.38 \times 10^{-9}$ m³kg⁻¹

2) Magnetization curves for low applied fields

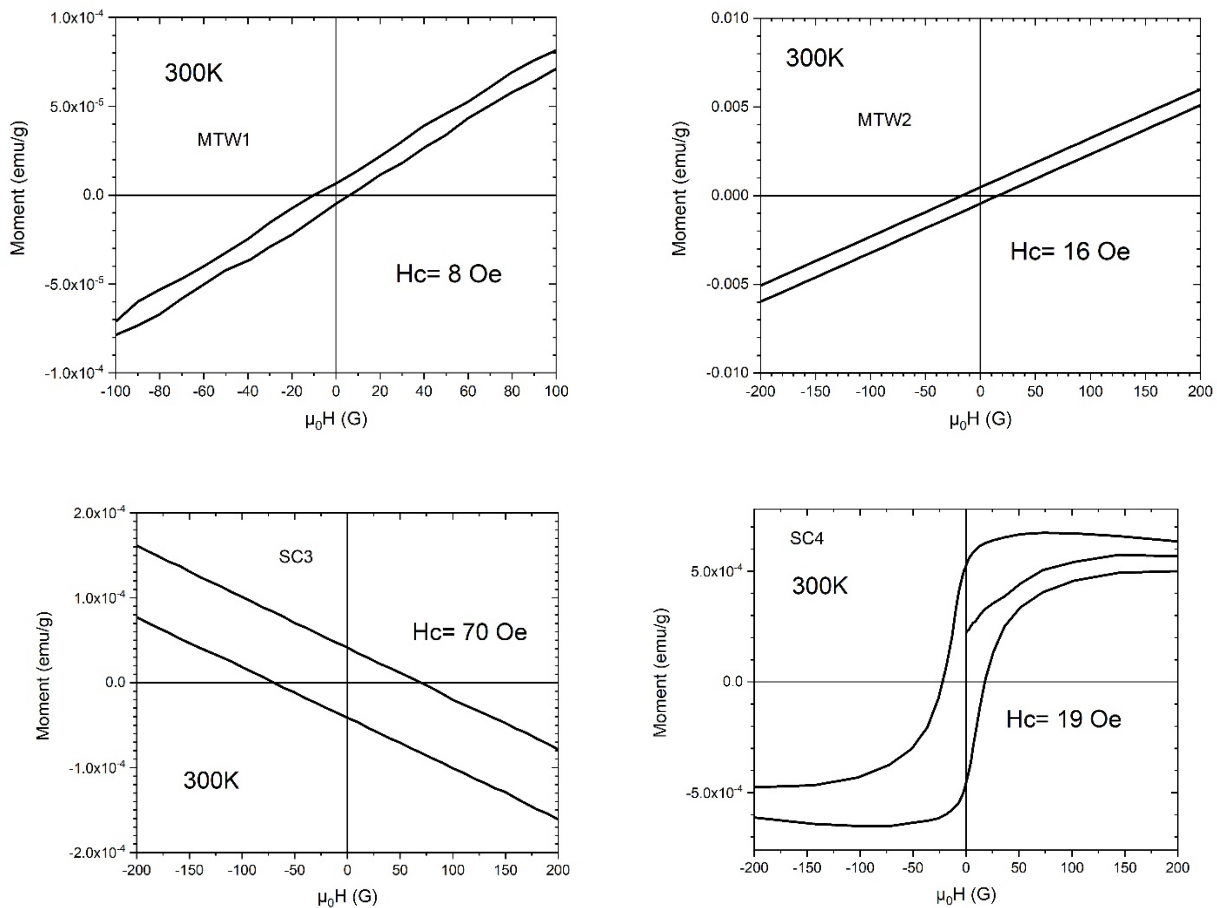


Figure S2. M(H) curves at low fields for multi-twinned nanoparticles (top row) and single-crystalline nanoparticles (bottom row).

3) Tentative fit of sample MTW2

A tentative has been made to adjust the magnetization curve of MTW2 with a Brillouin curve. Curves are shown below.

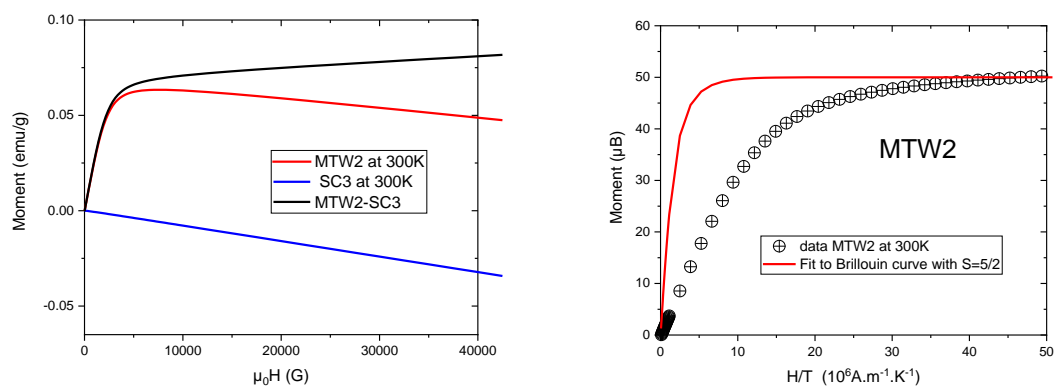


Figure S3. Raw data for MTW2 shows an important diamagnetic contribution which we have arbitrarily chosen to compensate by subtracting the almost purely diamagnetic behaviour of SC3 (leftmost figure). The data from the black curve have been used for fitting but all attempts to adjust the data with reasonable parameters failed (rightmost figure).